JOURNAL OF GEOPHYSICAL RESEARCH, VOL. 112, D10312, doi:10.1029/2006JD007826, 2007

Sensitivity of global sulphate aerosol production to changes in oxidant concentrations and climate

J. G. L. Rae,[1] C. E. Johnson,[1] N. Bellouin,[1] O. Boucher,[1] J. M. Haywood,[1] and A. Jones[1]

Received 2 August 2006; revised 12 January 2007; accepted 26 February 2007; published 25 May 2007.

[1] The oxidation of SO_2 to sulphate aerosol is an important process to include in climate models, and uncertainties caused by ignoring feedback mechanisms affecting the oxidants concerned need to be investigated. Here we present the results of an investigation into the sensitivity of sulphate concentrations to oxidant changes (from changes in climate and in emissions of oxidant precursors) and to changes in climate, in a version of HadGAM1 (the atmosphere-only version of HadGEM1) with an improved sulphur cycle scheme. We find that, when oxidants alone are changed, the global total sulphate burden decreases by approximately 3%, due mainly to a reduction in the OH burden. When climate alone is changed, our results show that the global total sulphate burden increases by approximately 9%; we conclude that this is probably attributable to reduced precipitation in regions of high sulphate abundance. When both oxidants and climate are changed simultaneously, we find that the effects of the two changes combine approximately linearly.

Citation: Rae, J. G. L., C. E. Johnson, N. Bellouin, O. Boucher, J. M. Haywood, and A. Jones (2007), Sensitivity of global sulphate aerosol production to changes in oxidant concentrations and climate, *J. Geophys. Res.*, *112*, D10312, doi:10.1029/2006JD007826.

1. Introduction

[2] It is important to improve the representation of aerosol species in climate models, as the level of confidence in aerosol predictions is still poor [*Ramaswamy et al.*, 2001]. Sulphate aerosol in the HadGEM1 climate model [*Martin et al.*, 2006; *Ringer et al.*, 2006; *Johns et al.*, 2006] is produced from reactions of dimethyl sulphide (DMS) and sulphur dioxide (SO_2) with gas- and aqueous-phase oxidants. These oxidant distributions are currently provided as prescribed fields; this method is similar to those used by *Feichter et al.* [2004] and *Pham et al.* [2005]. The oxidants in HadGEM1 are monthly mean fields with seasonal variations, obtained off-line from calculations with the STOCHEM chemistry model [described by *Collins et al.*, 1997 and *Stevenson et al.*, 1998], and do not vary with year, emissions scenario, or climate. Ideally, the oxidant concentrations should be calculated using an online tropospheric chemistry model and made available at each timestep, as in the works of *Berglen et al.* [2004] and *Unger et al.* [2006]. However, such online chemistry models are still expensive to include for all climate simulations. Their inclusion could lead to improved estimates of sulphate aerosol production because (1) variability of oxidants due to cloud amount, precipitation, and chemical precursors is modeled, and (2) changes due to long-term evolution of oxidant precursor emissions and climate are included. Here we investigate the importance of this second effect.

[3] Future oxidant concentrations will be determined primarily by changes in emission rates of precursors such as NO_x, CO, and CH_4. Climate change, through its effect on atmospheric temperatures and humidities, will also have an influence. It is therefore expected that tropospheric oxidant concentrations will vary with emissions scenario and with changing climate [e.g., *Johnson et al.*, 1999; *Liao et al.*, 2003; *Zeng and Pyle*, 2003; *Berglen et al.*, 2004]. These changes in oxidant concentrations will result in changes in the simulated concentrations of sulphate aerosol in the troposphere, so the assumption of invariance from one year to the next is invalid and needs to be reconsidered.

[4] The production of the oxidants responsible for sulphate generation starts with the following sequence:

$$O_3 + h\nu \rightarrow O(^1D) + O_2 \quad (1)$$

$$O(^1D) + H_2O \rightarrow 2OH. \quad (2)$$

OH reacts with CO, CH_4, and other hydrocarbons to produce HO_2. The reaction of OH with CH_4 is very sensitive to temperature: for a typical 1990–2100 change in annual mean temperature in Europe, the rate coefficient calculated from data in the International Union of Pure and Applied Chemistry (IUPAC) database (see http://www.iupac-kinetic.ch.cam.ac.uk/) increases by approximately 10%. H_2O_2 is produced in the reaction:

$$HO_2 + HO_2 \rightarrow H_2O_2. \quad (3)$$

This reaction is catalyzed by water vapor, and the rate coefficient is therefore dependent on specific humidity.

[1]Met Office, Hadley Centre for Climate Change, Exeter, Devon, UK.

0148-0227/07/2006JD007826$09.00

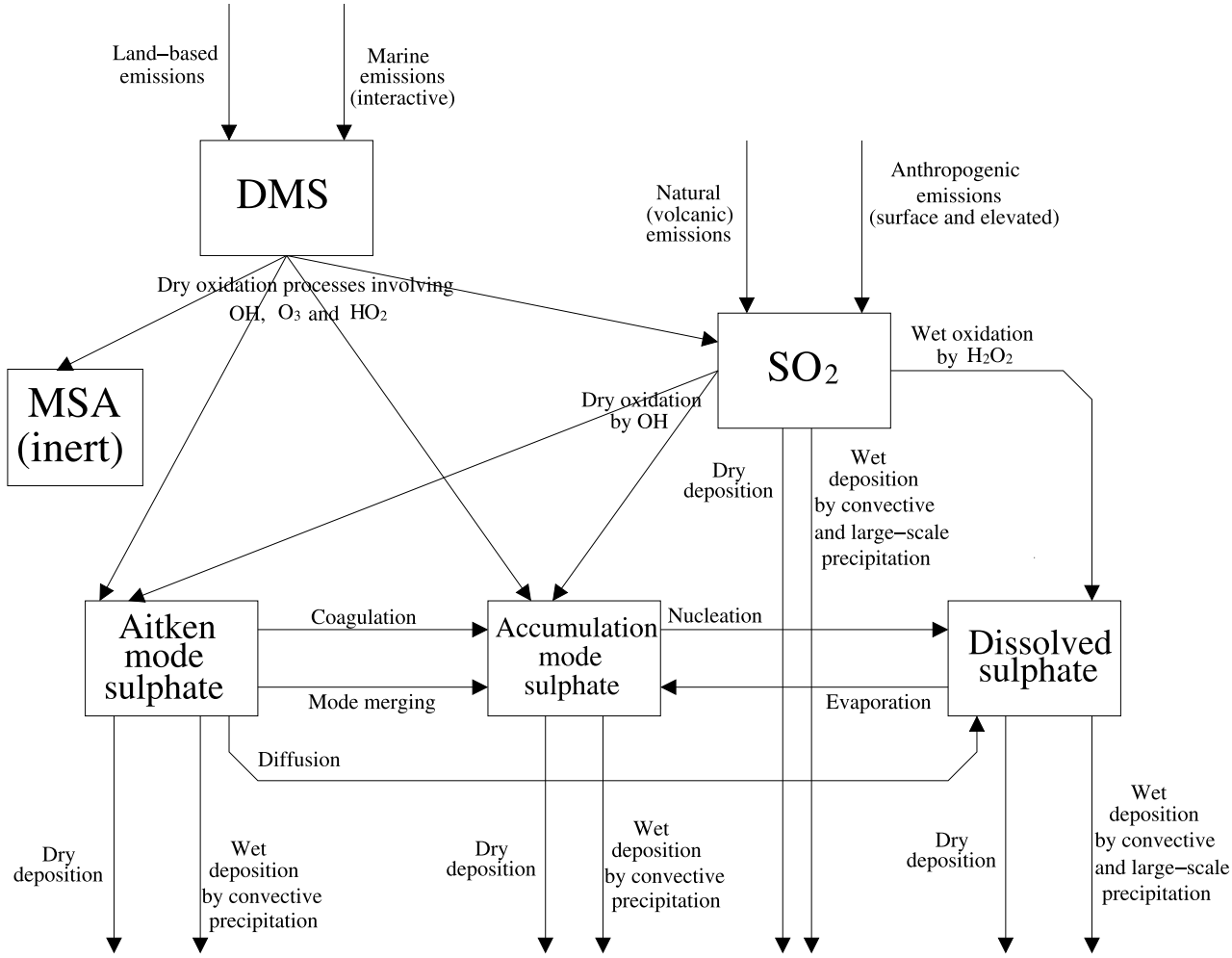

Figure 1. Schematic representation of the improved HadGEM1 sulphur-cycle scheme.

However, it also depends inversely on temperature, and our calculations have shown that, when climate conditions appropriate for the 2090s rather than the 1990s are used, the increase in the reaction rate caused by increasing specific humidity and the reduction caused by increasing temperature are of a similar order, resulting in only a very small change to the reaction rate on average.

[5] OH may be regenerated from the reactions of NO and O_3 with HO_2 and from the photolysis of oxidized products such as HCHO and H_2O_2. A detailed description of the chemistry affecting oxidant concentrations can be found in, e.g., the works of *Seinfeld and Pandis* [1998], *Finlayson-Pitts and Pitts* [2000], and in the IUPAC database. The rates of the gas-phase reactions depend on temperature. Both temperature and water vapor concentration will be affected by climate change. The O_3 concentration will also be affected by stratosphere-troposphere exchange, which in turn could also be influenced by changes to climate [*Collins et al.*, 2003; *Butchart and Scaife*, 2001]. The changes to oxidants as a result of climate change, together with emissions of oxidant precursors, have complex geographical and temporal variations [see, e.g., *Johnson et al.*, 1999, 2001; *Zeng and Pyle*, 2003].

[6] Climate change is also expected to affect sulphate aerosol generation directly through the effect of temperature changes on rates of gas-phase oxidation of DMS and SO_2 and the effect of changing cloud-water content and cloud amount on rates of aqueous-phase oxidation of SO_2. Precipitation changes may affect rates of wet deposition, and there could also be changes in long-range transport, resulting in different distributions of sulphate and its precursors.

[7] It can be seen, therefore, that future climate changes could influence sulphate aerosol production in many ways, both direct and indirect. Here we use HadGAM1, the atmosphere-only version of HadGEM1, to conduct a sensitivity study of the effect of changes in oxidant concentrations, resulting from climate and emission changes, on the sulphur cycle. In addition, we investigate the sensitivity of the sulphur cycle to the direct influence of climate change.

2. Sulphur Scheme

[8] The sulphur-cycle scheme in HadGEM1 is described in detail by *Jones et al.* [2001], and the improved scheme used by us is shown schematically in Figure 1. In the model, sulphate is present as three modes: Aitken, accumulation, and dissolved (in cloud droplets). The model has an interactive scheme for the emission of oceanic DMS [*Jones and Roberts*, 2004]. This scheme uses prescribed seasonally varying fields for DMS seawater concentrations, along with

winds and sea-surface temperatures from the model, to calculate rates of DMS emission. Three alternative parameterizations of sea-air exchange are provided; in this work, that of *Wanninkhof* [1992] was used. DMS is oxidized in a scheme involving OH, O_3, and HO_2 to produce SO_2, sulphate, and methanesulphonic acid (MSA). This scheme is parameterized in HadGEM1 [see *Jones et al.*, 2001 for further details]. The MSA produced in these reactions does not participate in any further processes in the model. SO_2 is oxidized by OH in the gas phase and by H_2O_2 in the aqueous phase to form sulphate. In the model, H_2O_2 is depleted by this reaction and replenished by reaction (3) above, up to a maximum equal to the value in the input field. The model does not currently include aqueous oxidation of SO_2 by O_3 or aqueous oxidation of sulphur oxides catalyzed by metals.

[9] While these reactions are important, the rates of oxidation by O_3 [*Seinfeld and Pandis*, 1998] and of oxidation catalyzed by iron [*Warneck et al.*, 1996] depend on pH, which in turn depends on the concentrations of many chemical species, and is therefore very difficult to calculate in a noncoupled model like ours. The inclusion of these reactions would lead to a lower SO_2 burden. This lower SO_2 burden may feed through to a lower sulphate burden due to less SO_2 being available for gas-phase oxidation by OH, but the aqueous reactions themselves would produce dissolved sulphate, which has a very short lifetime because of rapid wet scavenging. SO_2 and sulphate are subject to wet and dry deposition [see *Jones et al.*, 2001]. Several improvements were made to the sulphur cycle scheme of *Jones et al.* [2001] and are described below. As a result of these changes, modeled aerosol optical depths have increased significantly and now match observations more closely.

[10] The treatment of partitioning, into the Aitken and accumulation modes, of sulphuric acid, produced by gas-phase oxidation of SO_2 and DMS, was improved. Lookup tables were used to calculate, as functions of relative humidity, the condensation rates per molecule of gaseous sulphuric acid onto Aitken- and accumulation-mode sulphate. They are also functions of temperature and pressure, but these dependences are weak. The calculation of the numbers in the lookup tables was based on the condensation theory used in the Global Model of Aerosol Processes (GLOMAP) model [*Spracklen et al.*, 2005], under the assumption that H_2SO_4 is in steady state; that is, that the rate of condensation onto sulphate aerosol is equal to the rate of chemical production in the reaction of SO_2 with OH.

[11] An additional Aitken-accumulation mode-merging process was introduced to take account of the growth of Aitken-mode particles as a result of condensation. The Aitken and accumulation modes have a certain region of overlap (at a radius of about 7 nm). In the new mode-merging process, the fraction of Aitken-mode sulphate, which transfers to the accumulation mode in one timestep, was taken to be equal to the fraction which grows enough in one timestep that it transfers into this overlap region. In this way, a parameterization was developed in which the flux associated with this process is calculated as mass-mixing ratio per timestep and is directly proportional to the rate of production of Aitken-mode sulphate.

[12] The treatment of rainout of dissolved sulphate was changed to include the effect of precipitation evaporating before reaching the surface. Previously, the rainout rate of dissolved aerosol in a gridbox was assumed to be proportional to the amount of condensed water removed as precipitation in that gridbox. In the new rainout scheme, the aerosol rainout rate depends on the rate of conversion of condensed water to precipitation, and reevaporation is included via the transfer of sulphate from the dissolved mode to the accumulation mode with a mass flux proportional to the amount of precipitation that reevaporates. To take account of incomplete evaporation of droplets, we follow *Boucher et al.* [2002] in transferring only half of the dissolved sulphate mass in a gridbox to the accumulation mode unless all precipitation in that gridbox evaporates completely.

[13] The size distribution of the Aitken mode was also changed to one that reproduces observations more closely. The new distribution is based on the smallest lognormal distribution of urban environment aerosols given in Table 2 of *Jaenicke* [1993]. The revised distribution has median radius r_g = 6.5 nm and geometric standard deviation σ_g = 1.3. The size distribution of the accumulation mode was unchanged (median radius r_g = 0.095 μm, standard deviation σ_g = 1.4).

3. Model Experiments

[14] We ran HadGAM1 with the improved sulphur cycle at a resolution of 1.875° in longitude and 1.25° in latitude, with 38 vertical levels, for several scenarios with different inputs for oxidant concentrations and climate appropriate for the present day and for the 2090s. In all cases, we used present-day anthropogenic SO_2 emissions appropriate for the 1990s [*Smith et al.*, 2004], and three-dimensional natural (i.e., volcanic) SO_2 emissions from the inventory of *Andres and Kasgnoc* [1998]. In all scenarios, DMS emissions were allowed to vary according to the interactive scheme described in section 2.

[15] Climate boundary conditions in the form of sea ice fraction and surface temperature fields were obtained, from previous HadCM3-STOCHEM coupled model simulations, for the 1990s and for the 2090s, with Special Report on Emissions Scenarios (SRES) scenario A2 (see http://sres.ciesin.org/). Concentrations of atmospheric greenhouse gases (CO_2, CH_4, NO_2, CFC-11, and CFC-12) appropriate for the 1990s, and for the 2090s under SRES scenario A2, were used.

[16] Concentrations of OH, O_3, H_2O_2, and HO_2 were obtained from STOCHEM simulations for the year 1990, and for the year 2100 with SRES emissions scenario A2. In each case, emissions and climate boundary conditions appropriate for that year were used. Figure 2 shows column densities (i.e., column mass per unit surface area) of OH (Figure 2a) and H_2O_2 (Figure 2b) obtained for 1990 and percentage differences between column densities of these species for 1990 and those for 2100 (Figures 2c and 2d), where the percentage difference is calculated as $100 \times (\frac{2100-1990}{1990})$. The H_2O_2 concentration was greater in 2100 than in 1990 in all of the main areas in which SO_2 is abundant (Europe, eastern China, and the northeastern United States). The changes in OH were not so straightforward, with increases in some areas and on some model levels and decreases in others. Table 1 shows global total

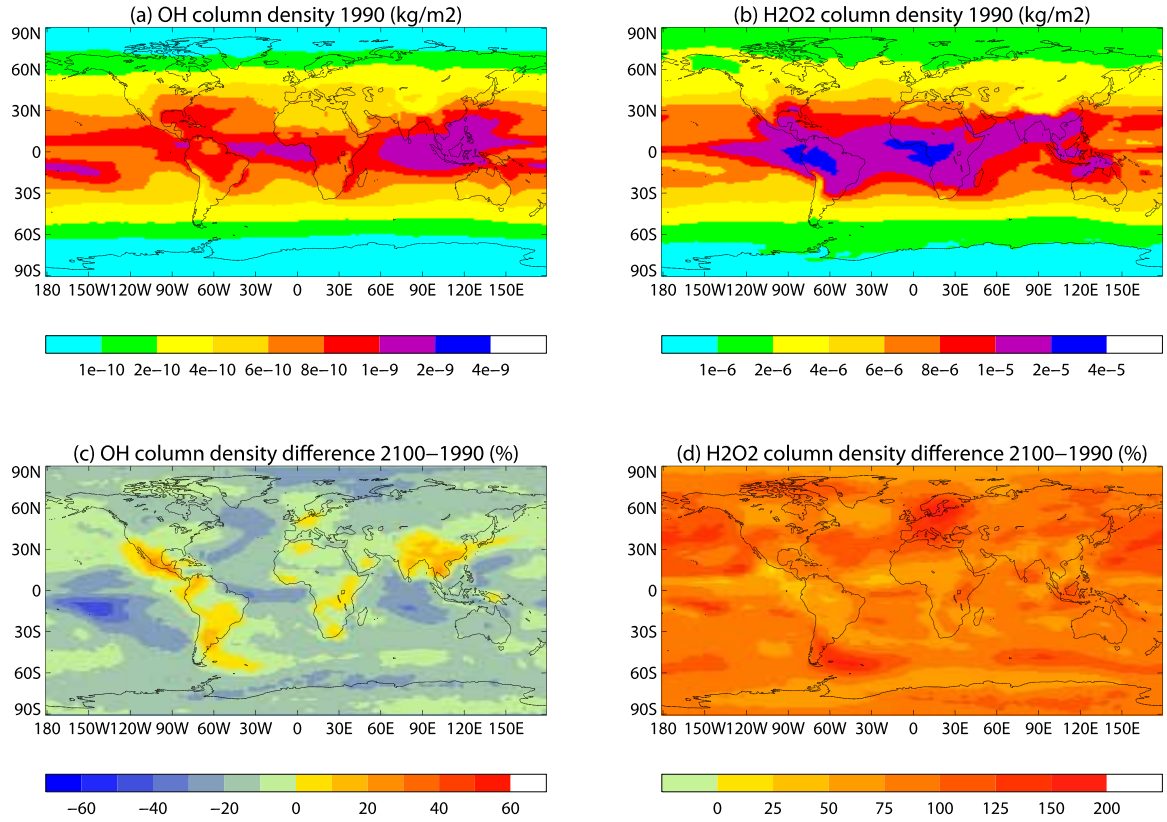

Figure 2. Oxidants: (a) annual mean OH column density (kg m^{-2}) in 1990; (b) annual mean H_2O_2 column density (kg m^{-2}) in 1990; (c) percentage difference in annual mean OH column density in 2100 relative to 1990; (d) percentage difference in annual mean H_2O_2 column density in 2100 relative to 1990.

tropospheric burdens of OH and H_2O_2 in 1990 and percentage differences between tropospheric burdens in 1990 and 2100. In 2100, the burden of OH is 12% lower, and that of H_2O_2 is 84% higher, than in 1990. The chemistry affecting OH and H_2O_2 was discussed in section 1. The changes in the concentrations of OH and HO_2 will normally have opposite signs to each other and, as H_2O_2 is formed from the reaction of HO_2 with itself, the change in H_2O_2 will normally be greater than, and have the opposite sign to, the change in OH. This is indeed what is observed here in the global total burdens of OH and H_2O_2.

[17] The sensitivity experiments are summarized in Table 2. For experiment CTRL (the control experiment), the oxidant distributions were calculated with 1990 emissions and climate boundary conditions. These oxidant distributions were then used with 1990s climate boundary conditions and greenhouse-gas concentrations in the calculation of the SO_2 and sulphate distributions. For experiment OXID, the oxidant distributions were calculated using projected 2100 emissions and climate boundary conditions. These oxidant distributions were then used with 1990s climate boundary conditions and greenhouse-gas concentrations in the calculation of the SO_2 and sulphate distributions. In experiment CLIM, we used the same oxidant distributions as in experiment CTRL, but with 2090s climate boundary conditions and greenhouse-gas concentrations, to calculate the SO_2 and sulphate distributions. In experiment BOTH, we used the same oxidant distributions as in experiment OXID and the same climate boundary conditions and greenhouse-gas concentrations as in experiment CLIM to calculate SO_2 and sulphate distributions. In each case, the HadGAM1 model with modified sulphur cycle was run for 5 years (1991–1995 or 2091–2095) after an initial spin-up period of 3 months.

4. Results and Discussion

[18] For each experiment, 5-year means have been calculated for the column densities of SO_2, the three modes of sulphate, and total sulphate. The tropospheric burdens for the control experiment (CTRL) are given in the second column of Table 3. Standard deviations in the 5-year means (calculated from the five separate annual means) are given in brackets. The final three columns of Table 3 give the percentage differences between the totals for this experiment and those for the three other experiments in Table 2, where the percentage difference is calculated as $100 \times (\frac{\text{OXID}-\text{CTRL}}{\text{CTRL}})$, etc. To determine the statistical significance of these results, we conducted a *t* test using the 5-year mean global total burdens and the standard deviations calculated

Table 1. Total Tropospheric Oxidant Burdens in 1990 and Percentage Differences Between These and Those in 2100 Relative to 1990

Species	1990 Burden (Tg)	Percentage Difference 2100–1990
OH	2.83×10^{-4}	−11.7
H_2O_2	3.39	+83.7

Table 2. Summary of Model Experiments

Experiment	Sea Ice, Sea Surface Temperatures, and Greenhouse-Gas Concentrations	Sulphur-Cycle Oxidant Concentrations
CTRL	1990s	1990
OXID	1990s	2100
CLIM	2090s	1990
BOTH	2090s	2100

from the five individual annual means. Statistical significance at the 5% level is indicated in Table 3. All of the results for SO_2 and total sulphate were found to be statistically significant at this level.

[19] The column densities of SO_2 and total sulphate (Aitken + accumulation + dissolved) from experiment CTRL and the percentage differences between these and the column densities from experiments OXID, CLIM, and BOTH are shown in Figure 3.

4.1. Effect of Oxidant Change Only (Experiment OXID)

[20] When the climate boundary conditions and greenhouse-gas concentrations are held at 1990s values and the oxidants are changed from 1990 values (experiment CTRL) to 2100 values (experiment OXID), the tropospheric burdens of SO_2 and total sulphate both decrease (Table 3). Total tropospheric production rates and mean tropospheric removal lifetimes (mass / loss rate) associated with some processes are given in Table 4 for the control scenario. Percentage differences (calculated in the same way as before) between the values for the control scenario and those for experiment OXID are also given. The decrease in the rate of production of Aitken-mode sulphate by dry oxidation of SO_2, responsible for about two thirds of Aitken-mode production, occurs because of the decrease in tropospheric OH burden seen in Table 1. The rate of oxidation of DMS, responsible for about one third of Aitken-mode production, increases because of increases in HO_2 and O_3 concentrations (not shown in Table 1), but this is dwarfed by the decrease in production by oxidation of SO_2. The result is a reduction of about 5% in the tropospheric Aitken-mode burden, which is statistically significant (Table 3). The 2% change in the accumulation-mode burden (Table 3) was not found to be statistically significant.

[21] In the control scenario, the lifetimes for removal of SO_2 via dry oxidation by OH and via aqueous oxidation by H_2O_2 are both of the order of 10 days (not shown in Table 4). In scenario OXID, the lifetime for removal of SO_2 via dry oxidation by OH increases by about 5%, while that for removal via aqueous oxidation by H_2O_2 decreases by about 20%. (Neither of these results is shown in Table 4, but they can be calculated from the changes in the burdens given in Table 3 and the changes in the rates given in Table 4.) The effect on SO_2 of the increase in H_2O_2 concentration therefore dominates over that of the decrease in OH concentration, and the SO_2 burden decreases. Using 5-year mean burdens and removal rates, the lifetime of dissolved-mode sulphate was calculated to be of the order of 1 hour, and those of the Aitken and accumulation modes were calculated to be approximately 30 hours and 12 days, respectively. In the case of the accumulation mode, the rate of removal by nucleation is almost balanced by the rate of production by evaporation, so in calculating the removal rate for this mode, we used the net rate (nucleation minus evaporation) instead of the nucleation rate itself. The dissolved mode has a shorter lifetime than the other two modes because it has a greater wet deposition rate in the model. Therefore much of the dissolved-mode sulphate produced by aqueous-phase oxidation of SO_2 is removed by wet scavenging, so that the increase in the dissolved mode is much smaller than the decrease in the other two modes combined, and the net effect is a decrease in total sulphate, as seen in Table 3. Therefore the effect on the total sulphate burden of the reduction in OH dominates over that of the increase in H_2O_2, despite the latter being more than seven times greater than the former.

[22] The last line of Table 4 gives the lifetime of total sulphate (Aitken, accumulation, and dissolved combined) for removal by all sink processes for the control experiment and the percentage differences between this and the lifetimes for the other experiments. In the case of experiment OXID, the lifetime decreases because, as discussed above, the oxidant changes result in more sulphate in the dissolved mode and less in the Aitken and accumulation modes. As the dissolved-mode lifetime is shorter than those of the other two modes, this results in a shorter lifetime for total sulphate.

[23] The geographical distribution of the changes in 5-year mean column density of SO_2 is shown in Figure 3c. There are increases over Scandinavia, northeast Africa, and part of the southern Pacific Ocean off the west coast of South America. The distribution of the changes in 5-year mean column density of total sulphate is shown in Figure 3d. There are increases over northern Europe, the Indian subcontinent, part of southern Africa, and parts of Central and South America. The regions of increased sulphate column density to the northeast of the Indian subcontinent and in

Table 3. Five-year Mean Global Total Tropospheric Burdens of SO_2, the Three Modes of Sulphate, and Total Sulphate From the Control Experiment (With Standard Deviations, Calculated From the Five Separate Annual Means, in Brackets) and Percentage Differences in Total Burdens From Other Experiments Relative to CTRL[a]

		Percentage Differences From CTRL		
Species	CTRL (SD) Tg[S]	OXID	CLIM	BOTH
SO_2	0.569 (0.026)	−7.9 (*)	−5.6 (*)	−13.0 (*)
Aitken-Mode Sulphate	0.092 (0.001)	−5.4 (*)	+4.0 (*)	−1.0
Accumulation-Mode Sulphate	0.371 (0.007)	−2.3	+10.8 (*)	+9.2 (*)
Dissolved-Mode Sulphate	0.018 (0.000)	+1.7 (*)	−2.9 (*)	−0.6
Total Sulphate	0.481 (0.008)	−2.6 (*)	+8.9 (*)	+6.8 (*)

[a]Asterisks beside the percentage differences indicate that a *t* test showed the difference to be statistically significant at the 5% level.

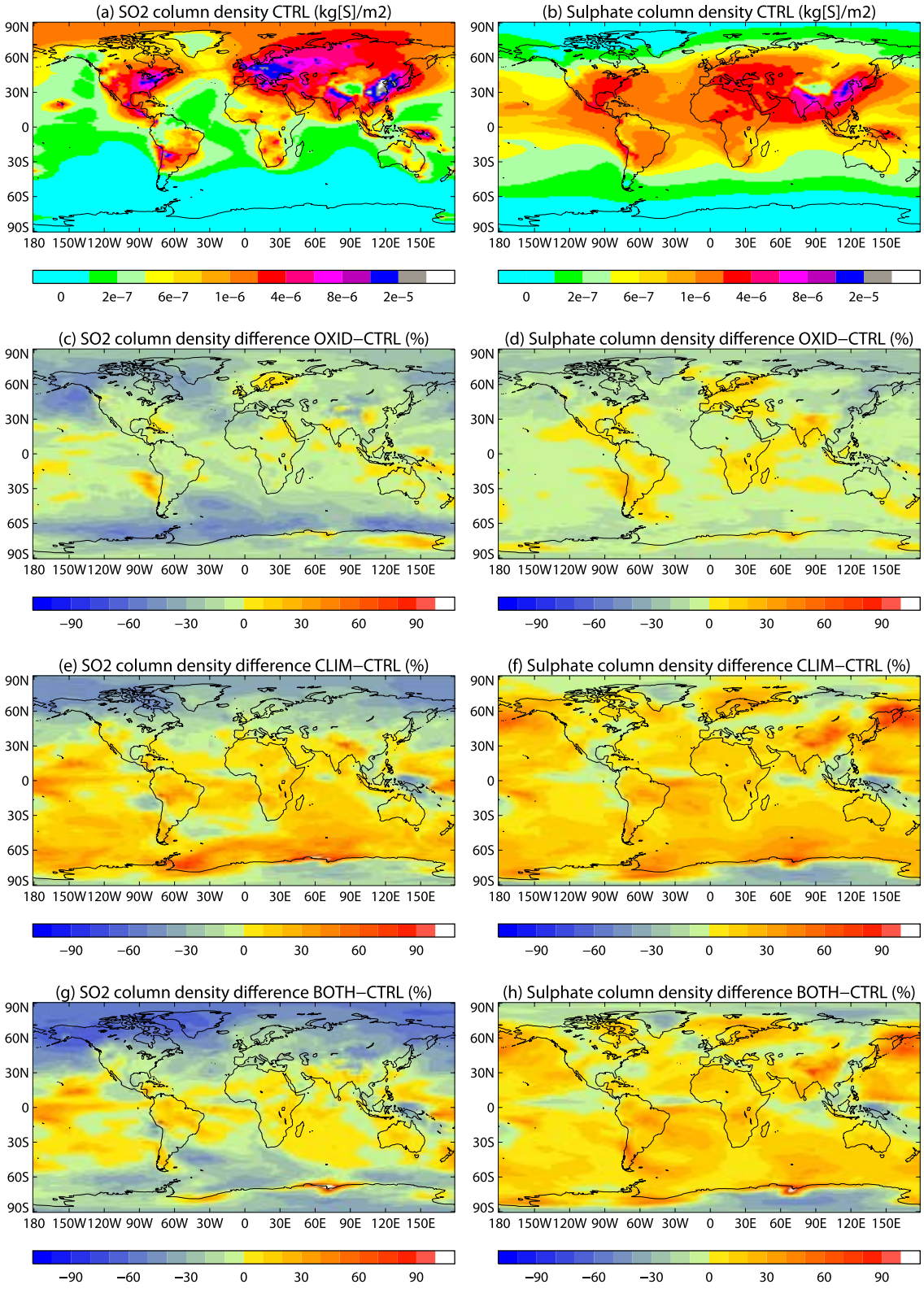

Figure 3. SO_2 and sulphate: (a) 5-year mean SO_2 column density (kg[S] m^{-2}) from CTRL; (b) 5-year mean total sulphate (Aitken + accumulation + dissolved) column density (kg[S] m^{-2}) from CTRL; (c) percentage difference in 5-year mean SO_2 column density in OXID relative to CTRL; (d) percentage difference in 5-year mean total sulphate column density in OXID relative to CTRL; (e) percentage difference in 5-year mean SO_2 column density in CLIM relative to CTRL; (f) percentage difference in 5-year mean total sulphate column density in CLIM relative to CTRL; (g) percentage difference in 5-year mean SO_2 column density in BOTH relative to CTRL; (h) percentage difference in 5-year mean total sulphate column density in BOTH relative to CTRL.

Table 4. Five-Year Mean Global Total Tropospheric Rates of Selected Production Mechanisms and Mean Tropospheric Lifetimes (Mass / Loss Rate) of Selected Removal Mechanisms and Percentage Differences Therein Relative to CTRL[a]

Quantity	CTRL	Percentage Differences From CTRL		
		OXID	CLIM	BOTH
Rate of Aitken Mode Production by Oxidation of SO_2 by OH	18.05 Tg[S]/yr	−13.3	−2.2	−14.4
Rate of Aitken Mode Production by Oxidation of DMS	8.36 Tg[S]/yr	+1.7	+3.6	+7.7
Rate of Accumulation Mode Production by Oxidation of SO_2 by OH	2.40 Tg[S]/yr	−9.6	+8.8	−2.1
Rate of Accumulation Mode Production by Oxidation of DMS	0.35 Tg[S]/yr	+8.0	+4.0	+16.7
Rate of Accumulation Mode Production by Coagulation of Aitken Mode	1.62 Tg[S]/yr	−5.6	+10.5	+3.7
Rate of Accumulation Mode Production by Mode Merging of Aitken Mode	9.94 Tg[S]/yr	−11.4	−0.4	−10.5
Rate of Dissolved Mode Production by Oxidation of SO_2 by H_2O_2	20.00 Tg[S]/yr	+15.5	−3.5	+12.0
Rate of Accumulation Mode Production From Dissolved Mode via Evaporation	75.00 Tg[S]/yr	+1.3	−0.7	+1.9
Rate of Accumulation Mode Production From Dissolved Mode via Reevaporation (Approximate)	18 Tg[S]/yr	0	−8	−6
Lifetime for Removal of Aitken Mode by Dry Deposition	32.6 days	−1.1	+0.6	−0.7
Lifetime for Removal of Aitken Mode via Scavenging by Convective Precipitation	12.3 days	−2.4	+0.3	−2.2
Lifetime for Removal of Aitken Mode by Mode Merging to Accumulation Mode	3.4 days	+6.8	+4.4	+10.5
Lifetime for Removal of Aitken Mode by Coagulation to Accumulation Mode	20.8 days	+0.3	−5.8	−4.5
Lifetime for Removal of Aitken Mode by Diffusion Into Cloud Droplets	3.1 days	+2.9	+7.0	+8.8
Lifetime for Removal of Accumulation Mode by Dry Deposition	73.8 days	−1.7	+0.5	+0.6
Lifetime for Removal of Accumulation Mode via Scavenging by Convective Precipitation	13.8 days	−0.5	+2.9	+1.9
Lifetime for Removal of Accumulation Mode via Nucleation to Form Dissolved Mode	1.4 days	−1.9	+13.8	+10.9
Lifetime for Removal of Dissolved Mode by Dry Deposition	3.9 days	−1.0	+6.5	+7.4
Lifetime for Removal Of Dissolved Mode via Scavenging by Convective Precipitation	9.5 days	−1.7	−11.0	−12.7
Lifetime for Removal of Dissolved Mode via Scavenging by Large-Scale Precipitation	0.2 days	−0.9	+1.2	+0.7
Lifetime for Removal of Total Sulphate by All Deposition Processes	3.5 days	−3.7	+9.7	+5.7

[a]The rate of transfer from dissolved to accumulation mode due to re-evaporation of falling precipitation is not diagnosed explicitly in the model and is therefore only known approximately.

Central and South America coincide with regions of increase of OH. The decreases in sulphate are mainly in Arctic and Antarctic regions. Sulphate does not always increase in regions where SO_2 decreases, and vice versa.

[24] In section 5 of their paper, *Pham et al.* [2005] gave the results of a study of the sensitivity of sulphate aerosol burdens to changes in oxidant concentrations. Using the Laboratoire de Météorologie Dynamique global climate model (GCM), they ran two experiments; both used 2100 SRES A2 sulphur emissions, but one used oxidant concentrations appropriate for the year 2000, and the other used oxidant concentrations appropriate for the year 2100 in SRES scenario A2. They found that the global burden of SO_2 decreased by 4–5% (whereas we found the decrease to be around 8%), while that of sulphate decreased by less than 1% (as opposed to the decrease of around 3% which we found). They attributed this small decrease to a more efficient oxidation, which results in sulphate being near the surface where it is scavenged and deposited more efficiently.

[25] *Unger et al.* [2006] ran simulations with the Goddard Institute for Space Sciences (GISS) ModelE general circulation model, with fully interactive chemistry and aerosols, for several model scenarios. For 2030s climate boundary conditions and emissions of sulphate precursors appropriate for 2030 in SRES scenario A1B, they ran simulations with emissions of O_3 precursors (which are also the precursors of sulphur-cycle oxidants such as OH and H_2O_2) for (1) 1995 from the EDGAR3.2 database (Simulation 2030SO_4) and (2) 2030 with SRES scenario A1B (Simulation 2030C). They studied the effect on sulphate burden at a regional scale and found that, over India and China, the rate of gas-phase oxidation of SO_2 was 21% higher with (2) than with (1), while the rate of aqueous oxidation was 5% lower over India and 4% lower over China. This resulted in sulphate burdens which were 8% and 7% higher over India and China, respectively. Because of reductions over Europe and the USA, they found that, globally, the rate of gas-phase oxidation increased by only 7%. They found the rate of aqueous oxidation to be unchanged globally, and their global total sulphate burden increased by only about 1% (as opposed to our decrease of about 3%). These changes in gas-phase oxidation rate and sulphate burden have the opposite signs to those which we found in our work with SRES scenario A2 in the 2090s (see Table 4). From the chemistry described in section 1, it can be seen that the balance between OH and H_2O_2 depends on the concentrations of species such as NO, O_3, CO, and hydrocarbons like CH_4; the concentrations of these species are in turn dependent on emissions of CH_4, NO_x, and CO. *Unger et al.* [2006] give the global increases in emissions between 1995 and 2030 for scenario A1B as 25% for CO, 33% for CH_4, and 80% for NO_x. In scenario A2 used by us, between 1990 and 2100, global total CO emissions increase by 165%, global total CH_4 emissions increase by 187%, and global total NO_x emissions increase by 252% [*Nakićenović et al.*, 2000]. These differences in the changes to emission rates of oxidant precursors between our work and that of Unger et al. will result in differences in the balance between OH and H_2O_2, leading to differences in the evolution of sulphate concentrations.

4.2. Effect of Climate Change Only (Experiment CLIM)

[26] The changes in tropospheric burdens of SO_2, total sulphate, and the three modes of sulphate, when the oxidant concentrations are held at 1990 values and the climate boundary conditions and greenhouse-gas concentrations are changed from 1990s (experiment CTRL) to 2090s (experiment CLIM) values, are given in Table 3. They are all statistically significant. The burdens of SO_2 and dissolved sulphate decrease, while those of the Aitken and accumulation modes increase. Again, the total sulphate is

dominated by the Aitken and accumulation modes and therefore increases.

[27] Percentage differences between the control experiment and experiment CLIM are given in Table 4 for total tropospheric production rates and mean tropospheric removal lifetimes associated with some selected processes. There are no significant changes in the lifetimes for removal of Aitken-mode sulphate by wet scavenging and dry deposition, but the increase in the Aitken-mode burden can be explained by several other factors. There is an increase in the rate of formation of Aitken-mode sulphate by oxidation of DMS. As this channel accounts for about one third of Aitken-mode production in the model, it is an important production mechanism. In addition, the lifetime for removal of Aitken-mode sulphate by mode merging to form accumulation-mode sulphate and that for removal by diffusion into cloud droplets also increase. In combination, these changes result in an increase of about 4% in the Aitken-mode burden (Table 3). The increase of 11% in the burden of accumulation-mode sulphate is due mainly to increases in the rates of production via gas-phase oxidation of SO_2 by OH and via coagulation of Aitken-mode particles, which in the control scenario are responsible for 17% and 12%, respectively, of accumulation-mode sulphate in the model if production by evaporation is ignored (production by evaporation is more than balanced by removal by nucleation, resulting in a net removal). Other factors which may have an effect are increases in the rate of production from oxidation of DMS and in the mean lifetime for removal of accumulation-mode sulphate by wet scavenging. There is no significant change in the lifetime for removal of accumulation-mode sulphate by dry deposition. In the case of both Aitken- and accumulation-mode sulphate, there was an increase in the rate of production via oxidation of DMS because the climate affects the rate of emission of DMS through the interactive scheme described in section 2. There was an increase in the global total DMS emission rate when climate boundary conditions and greenhouse-gas concentrations appropriate for the 2090s, rather than the 1990s, were used (not shown in Table 4).

[28] Table 4 also shows that the lifetime for removal of total sulphate was greater in experiment CLIM than in experiment CTRL. This increase is caused by reduced precipitation in regions where sulphate is abundant, particularly over India, the Middle East, and the eastern Mediterranean. There is also an increase in the lifetime of dissolved sulphate due to dry deposition, but this lifetime is still very short compared with those of the other two modes, so the effect on the lifetime of total sulphate is likely to be small.

[29] The geographical distribution of the percentage changes in SO_2 is shown in Figure 3e. The main increase is over the Southern Ocean, and there is a general decrease over much of the Northern Hemisphere. It is this decrease over the Northern Hemisphere, where SO_2 is most abundant (as can be seen from Figure 3a), that results in the decrease in global total SO_2 as given in Table 3. There is also a decrease over the Maritime Continent and a slight decrease over Antarctica.

[30] The distribution of the percentage change in total sulphate column density is shown in Figure 3f. It decreases in many of the places where SO_2 column density decreases (for example over the Arctic, the Antarctic, and the Maritime Continent). The large increase in the column density of total sulphate over the north Pacific Ocean occurs close to an area of increased DMS emission in the model, while the increase over China coincides with a region in which the model gives reduced precipitation. The increases over the Southern Ocean, although large in percentage terms, are actually numerically small, as the column density in scenario CTRL is small in this region (See Figure 3b), but are probably caused by increases in DMS emissions in this region.

[31] *Feichter et al.* [2004] used the fourth-generation Max Planck Institute for Meteorology general circulation model, ECHAM4-T30, to study the effects of changing greenhouse-gas concentrations and emissions of aerosols and their precursors from preindustrial to present-day values. They found that with present-day aerosol and aerosol precursor emissions, the global total aerosol burden was less with present-day than with preindustrial greenhouse-gas concentrations. They attribute this to the hydrological cycle being stronger with present-day greenhouse-gas concentrations, resulting in a shorter residence time for aerosols. Here we found that a change to future climate resulted in an increase of about 9% in the tropospheric sulphate burden; this is at least partly due to greater DMS emissions and subsequent oxidation of DMS to SO_2 and sulphate. If there was no change to the deposition process, then one would expect a corresponding increase in the deposition rate. The global total precipitation in scenario CLIM is about 8% greater than in scenario CTRL, so for this reason too, one would expect an increase in the deposition rate. However, in fact the rate of removal of total sulphate by wet scavenging decreases very slightly by about 1% (although this change is probably too small to be significant). So despite an increase of 9% in the global total sulphate burden and an increase of about 8% in the global total precipitation, the rate of removal of sulphate by wet scavenging is almost unchanged. This appears to be due to geographical effects; that is, increased deposition in some regions is balanced by reduced deposition in others.

4.3. Combined Effect of Oxidant and Climate Changes (Experiment BOTH)

[32] Table 3 gives the tropospheric changes in SO_2, total sulphate, and the three modes of sulphate when oxidant concentrations are changed from 1990 values to 2100 values and climate boundary conditions and greenhouse-gas concentrations are changed from 1990s values to 2090s values. It can be seen that the changes due to future oxidant concentrations and future climate add approximately linearly in all statistically significant cases.

5. Conclusions

[33] We have studied the sensitivity of SO_2 and sulphate to future oxidant concentrations and future climate changes. Oxidant concentrations were changed from 1990 values (experiment CTRL) to 2100 values (experiment OXID). The total tropospheric OH (responsible for gas-phase oxidation of SO_2 to Aitken- and accumulation-mode sulphate) decreased by around 12%, while the total H_2O_2 (responsible for aqueous-phase oxidation of SO_2 to dissolved sulphate)

increased by more than 80%. This resulted in a decrease of 8% in the tropospheric burden of SO_2 and a decrease of 3% in that of sulphate. There was a decrease of 5% in Aitken-mode sulphate and an increase of 2% in dissolved sulphate. A *t* test showed all of these results to be statistically significant at the 5% level; however, the change in accumulation-mode sulphate was not statistically significant.

[34] The decrease in SO_2 can be explained by the increase in H_2O_2 and by the fact that aqueous-phase oxidation dominates over gas-phase. The sulphate produced in this way is in the dissolved mode, which has a very short lifetime due to wet deposition. The total sulphate burden in the model is dominated by the Aitken and accumulation modes, which are produced by gas-phase oxidation of SO_2 by OH, so decreasing total OH reduces total sulphate.

[35] We also looked at the effect of changing the climate inputs from 1990s values (experiment CTRL) to 2090s values (experiment CLIM). In this case, there was a decrease of 6% in tropospheric SO_2 burden and an increase of 9% in tropospheric sulphate burden. The Aitken- and accumulation-mode burdens increased by 4% and 11%, respectively. The dissolved-mode burden decreased by 3%, but the contribution of this mode to the total sulphate burden is very small. The increases in the burdens of the Aitken and accumulation modes can probably be attributed to reduced precipitation in regions where sulphate is abundant. All of these results were found to be statistically significant at the 5% level.

[36] When oxidant concentrations and climate were changed simultaneously (experiment BOTH), the percentage changes in tropospheric burdens of SO_2 and total sulphate were found to be statistically significant and were approximately equal to the sums of the percentage changes due to oxidant changes and those due to climate changes. The changes in Aitken mode and dissolved-mode sulphate were not statistically significant. The change in accumulation-mode sulphate was statistically significant, but it is not possible to draw any conclusions about it in relation to the results of the other scenarios, as the result in scenario OXID was not statistically significant.

[37] We did not consider the effect of changing sulphur-cycle emissions. These are likely to be the dominant influence on future sulphate concentrations, but we consider that it is also important to include future changes in climate and oxidant concentrations in model calculations. In addition, the SRES scenarios for SO_2 emissions are not necessarily realistic. We therefore chose to restrict our work to the sensitivity of sulphate concentrations to changes in climate and oxidants only.

[38] In this study, we used emissions of oxidant precursors for the year 2100 in SRES scenario A2. As stated in the previous paragraph, the realism of the SRES scenarios is unclear; in addition, the scenarios are based on predictions of future global economic development, and it is difficult to say whether one scenario is more likely to occur than another. A2 is one of the scenarios with the greatest increase in the global total emissions of oxidant precursors and greenhouse gases between 2000 and 2100. This is in contrast to, for example, scenario B1, which shows emissions peaking around the middle of the century before starting to decrease, so that by 2100, the global total emission rates of these species are generally less than they were in 2000. The emission rates of species such as NO_x and CH_4 will affect the balance between OH and HO_2 and will therefore affect the concentrations and distributions of OH and H_2O_2. However, the reaction system is complex, and without carrying out model experiments, it is difficult to predict the effect of using one SRES scenario as opposed to another.

[39] We have shown that, both globally (Table 3) and regionally (Figure 3), the effect of oxidant changes on sulphate aerosol concentrations is of comparable magnitude to that of climate changes. It is therefore important that the variation of oxidant concentrations with changes in emissions and climate is included in sulphate aerosol models. Such variations are of course included in fully coupled models such as those used by *Berglen et al.* [2004] and *Unger et al.* [2006]. A fully coupled model would obviously include instantaneous feedbacks from the sulphur cycle and meteorology on the oxidant concentrations, and this would have an effect on the results of a study such as this.

[40] Few studies address the effects of changing oxidant distributions on future sulphate aerosol concentrations, and those that do show diverging results. To reduce the uncertainty in predicted sulphate aerosol concentrations, it is important that we also improve our understanding of the role of oxidants in aerosol formation and the interaction of clouds with sulphate aerosol.

[41] **Acknowledgments.** We thank the reviewers for their helpful comments, which have led to significant improvements in this paper. This work was supported by the UK Department for Environment, Food and Rural Affairs under the Climate Prediction Programme, contract PECD 7/12/37.

References

Andres, R. J., and A. D. Kasgnoc (1998), A time-averaged inventory of subaerial volcanic sulfur emissions, *J. Geophys. Res.*, *103*, 25,251–25,261.

Berglen, T. F., T. K. Berntsen, I. S. A. Isaksen, and J. K. Sundet (2004), A global model of the coupled sulfur/oxidant chemistry in the troposphere: The sulfur cycle, *J. Geophys. Res.*, *109*, D19310, doi:10.1029/2003JD003948.

Boucher, O., M. Pham, and C. Venkataraman (2002), Simulation of the atmospheric sulfur cycle in the Laboratoire de Météorologie Dynamique general circulation model: Model description, model evaluation, and global and European budgets, *Note Sci. IPSL 23*, 27 pp., Inst. Pierre Simon Laplace, Paris, France (Available at http://www.ipsl.jussieu.fr/poles/Modelisation/NotesSciences.htm.)

Butchart, N., and A. A. Scaife (2001), Removal of chlorofluorocarbons by increased mass exchange between the stratosphere and troposphere in a changing climate, *Nature*, *410*, 799–802.

Collins, W. J., D. S. Stevenson, C. E. Johnson, and R. G. Derwent (1997), Tropospheric ozone in a global-scale three-dimensional model and its response to NO_x emission controls, *J. Atmos. Chem.*, *26*, 223–274.

Collins, W. J., R. G. Derwent, B. Garnier, C. E. Johnson, M. G. Sanderson, and D. S. Stevenson (2003), Effect of stratosphere–troposphere exchange on future tropospheric ozone trend, *J. Geophys. Res.*, *108*(D12), 8528, doi:10.1029/2002JD002617.

Feichter, J., E. Roeckner, U. Lohmann, and B. Liepert (2004), Nonlinear aspects of the climate response to greenhouse gas and aerosol forcing, *J. Climate*, *17*, 2384–2398.

Finlayson-Pitts, B. J., and J. N. Pitts (2000), *Chemistry of the Upper and Lower Atmosphere*, Elsevier, New York.

Jaenicke, R., (1993), Tropospheric aerosols, in *Aerosol–Cloud–Climate Interactions*, edited by P. V. Hobbs, pp. 1–31, Elsevier, New York.

Johns, T. C., et al. (2006), The new Hadley Centre climate model HadGEM1: Evaluation of coupled simulations, *J. Climate*, *19*, 1327–1353.

Johnson, C. E., W. J. Collins, D. S. Stevenson, and R. G. Derwent (1999), Relative roles of climate and emissions changes on future tropospheric oxidant concentrations, *J. Geophys. Res.*, *104*(D15), 18,631–18,645.

Johnson, C. E., D. S. Stevenson, W. J. Collins, and R. G. Derwent (2001), Role of climate feedback on methane and ozone studied with a coupled ocean–atmosphere-chemistry model, *Geophys. Res. Lett.*, *28*(9), 1723–1726.

Jones, A., and D. L. Roberts, (2004), An Interactive DMS Emissions Scheme for the Unified Model, *Hadley Centre Technical Note 47*, Met Office, Exeter, UK. (Available at http://www.metoffice.gov.uk/research/hadleycentre/pubs/HCTN/index.html)

Jones, A., D. L. Roberts, M. J. Woodage, and C. E. Johnson (2001), Indirect sulphate aerosol forcing in a climate model with an interactive sulphur cycle, *J. Geophys. Res.*, *106*, 20,293–20,310.

Liao, H., P. J. Adams, S. Chung, J. H. Seinfeld, L. J. Mickley, and D. J. Jacob (2003), Interactions between tropospheric chemistry and aerosols in a unified general circulation model, *J. Geophys. Res.*, *108*(D1), 4001, doi:10.1029/2001JD001260.

Martin, G. M., M. A. Ringer, V. D. Pope, A. Jones, C. Dearden, and T. J. Hinton (2006), The physical properties of the atmosphere in the new Hadley Centre Global Environmental Model, HadGEM1. Part 1: Model description and global climatology, *J. Climate*, *19*, 1274–1301.

Nakićenović, N., et al. (Eds.) (2000), Special report on emissions scenarios, *Special Report of Working Group III of the Intergovernmental Panel on Climate Change*, Cambridge Univ. Press, New York.

Pham, M., O. Boucher, and D. Hauglustaine (2005), Changes in atmospheric sulfur burdens and concentrations and resulting radiative forcings under IPCC SRES emission scenarios for 1990–2100, *J. Geophys. Res.*, *110*, D06112, doi:10.1029/2004JD005125.

Ramaswamy, V., et al. (2001), Radiative forcing of climate change, in *Climate Change 2001: The Scientific Basis. Contribution of Working Group I to the Third Assessment Report of the Intergovernmental Panel on Climate Change*, edited by J. T. Houghton, Y. Ding, D. J. Griggs, M. Noguer, P. J. van der Linden, X. Dai, K. Maskell, and C. A. Johnson, pp. 349–416, Cambridge Univ. Press, New York.

Ringer, M. A., et al. (2006), The physical properties of the atmosphere in the new Hadley Centre Global Environmental Model, HadGEM1. Part 2: Aspects of variability and regional climate, *J. Climate*, *19*, 1302–1326.

Seinfeld, J. H., and S. N. Pandis (1998), *Atmospheric Chemistry and Physics: From Air Pollution to Climate Change*, John Wiley, Hoboken, N. J.

Smith, S. J., R. Andres, E. Conception, and J. Lurz (2004), Historical sulfur dioxide emissions 1850–2000: Methods and results, *PNNL Research Report PNNL-14537*.

Spracklen, D. V., K. J. Pringle, K. S. Carslaw, M. P. Chipperfield, and G. W. Mann (2005), A global off-line model of size-resolved aerosol microphysics: I. Model development and prediction of aerosol properties, *Atmos. Chem. Phys.*, *5*, 2227–2252.

Stevenson, D. S., W. J. Collins, C. E. Johnson, and R. G. Derwent (1998), Intercomparison and evaluation of atmospheric transport in a Lagrangian model (STOCHEM) and an Eulerian model (UM), using ^{222}Rn as a short-lived tracer, *Q. J. R. Meteorol. Soc.*, *124*, 2477–2491.

Unger, N., D. T. Shindell, D. M. Koch, and D. G. Streets (2006), Cross influences of ozone and sulphate precursor emissions changes on air quality and climate, *Proc. Natl. Acad. Sci. USA*, *103*, 4377–4380.

Wanninkhof, R. (1992), Relationship between wind speed and gas exchange over the ocean, *J. Geophys. Res.*, *97*, 7373–7382.

Warneck, P., et al. (1996), Review of the activities and achievements of the EUROTRAC subproject HALIPP, in *Heterogeneous and Liquid-Phase Processes*, edited by P. Warneck, pp. 7–26, Springer, New York.

Zeng, G., and J. A. Pyle (2003), Changes in tropospheric ozone between 2000 and 2100 modeled in a chemistry-climate model, *Geophys. Res. Lett.*, *30*(7), 1392, doi:10.1029/2002GL016708.

N. Bellouin, O. Boucher, J. M. Haywood, C. E. Johnson, A. Jones, and J. G. L. Rae, Met Office, Hadley Centre for Climate Change, FitzRoy Road, Exeter, Devon, EX1 3PB, UK. (jamie.rae@metoffice.gov.uk)